Article

Methanol chemoreceptor MtpA- and flagellin protein FliC-dependent methylotaxis determines the spaciotemporal colonization of PPFM in the phyllosphere

Shiori Katayama[1], Kosuke Shiraishi[1], Kanae Kaji[1], Kazuya Kawabata[1], Naoki Tamura[2], Akio Tani[3], Hiroya Yurimoto[1*] and Yasuyoshi Sakai[1]

[1] Graduate School of Agriculture, Kyoto University, Kitashirakawa-Oiwake, Sakyo-ku, Kyoto, Japan

[2] Department of Anatomy and Histology, Fukushima Medical University School of Medicine, Hikarigaoka, Fukushima, Japan

[3] Institute of Plant Science and Resources, Okayama University, Okayama, Japan

Correspondence:

Hiroya Yurimoto

Division of Applied Life Sciences, Graduate School of Agriculture, Kyoto University, Kitashirakawa-Oiwake, Sakyo-ku, Kyoto 606-8502, Japan.

Phone: +81-75-753-6387

Fax: +81-75-753-6454

E-mail: yurimoto.hiroya.5m@kyoto-u.ac.jp

Keywords

PPFM, methylotaxis, phyllosphere, fluorescence imaging, bacterial behavior, plant-microbe interaction

Abstract

Pink-pigmented facultative methylotrophs (PPFMs) capable of growth on methanol are dominant and versatile phyllosphere bacteria that provide positive effects on plant growth through symbiosis. However, the spatiotemporal behavior of PPFMs on plant surfaces and its molecular basis are unknown. Here we show that *Methylobacterium* sp. strain OR01 inoculated onto red perilla seeds colonized across the entire plant surface in the phyllosphere concomitant with the plant growth. FliC flagellin proteins required for motility were necessary for distributed colonization on plant leaves, but not for colonization at the leaf periphery. Methanol-sensing chemoreceptor MtpA-dependent chemotaxis (methylotaxis; chemotaxis toward methanol) facilitated the bacterial movement from the peripheral to the inner part of leaves and further entry into the stomatal cavity, indicating that methanol functions as a volatile messenger attracting PPFMs to particular leaf locations possibly to support with photosynthesis and to afford protection from pathogenic invasion.

Methylobacterium sp., referred to as pink-pigmented facultative methylotroph (PPFM), is one of the most ubiquitous and abundant bacterial genera present in the aerial parts of the plant, the phyllosphere. PPFM is estimated to exist at 10^4–10^7 colony forming units (CFU) per gram fresh weight of plant materials[1]. Many strains of *Methylobacterium* are known for their ability to promote plant growth through the production of plant hormones such as auxins and cytokinin, and to induce systemic resistance to pathogens and diseases[2-7]. In turn, they obtain nutrients from the host plant, establishing the symbiotic relationship in the phyllosphere.

Methylobacterium species phylogenetically close to *Methylobacterium* sp. strain OR01 is observed on red perilla seeds and leaves collected from various regions of Japan[8], indicating that this species is the major colonizer of red perilla leaves. Such species-level specificity of the interaction between the red perilla plant and strain OR01 makes them an ideal system for investigating the ecology and physiology of PPFMs in the phyllosphere. The factors and features that contribute to strain OR01 attaining the dominant colonizer status of perilla phyllosphere still remain unknown and need to be elucidated.

Even though the phyllosphere is speculated to be nutrient-poor, plants indeed provide nutrient compounds sufficient to sustain large microbial communities[9]. In particular, methanol, produced from the cell wall component pectin, is recognized as a relatively abundant carbon source for methanol-utilizing microorganisms[10], which proves advantageous for PPFMs and allows them to dominate the phyllosphere[11]. PPFMs have developed several survival strategies to help them adapt to the harsh and ever-changing phyllosphere environment, brought about by various factors such as UV, temperature, osmotic and oxidative stresses[12]. In *Methylorubrum extorquens* AM1, the KaiC protein, a homologue of the cyanobacterial circadian protein, has been shown to facilitate colonization in the phyllosphere through a concerted regulation of environmental responses towards UV and temperature[13]. Previously, we revealed a periodic fluctuation in methanol concentration on *Arabidopsis* leaves, i.e. high in the dark period and low in the light period, using a yeast methanol sensor that could directly measure methanol concentrations[14]. We also showed that in response to these diurnal changes in methanol concentration, the methanol-utilizing yeast *Candida boidinii* regulates its gene expression and peroxisome homeostasis necessary for methanol metabolism.

Chemotaxis, the movement of bacteria as a response to chemical stimulus, is driven by three main components: methyl-accepting chemotaxis proteins (MCPs) as sensor chemoreceptors, Che proteins as transmitters of chemotactic signals through

phosphorylation, and flagellum as the driving force of directed movement[15, 16] (cf. Fig. 4A). Our recent study on *Methylobacterium aquaticum* strain 22A showed that three MCPs (MtpA, MtpB and MtpC) were responsible for chemotaxis toward methanol, methylotaxis[17]. A triple *M. aquaticum* strain 22A mutant of these MCPs lost methylotaxis and showed less efficient colonization on plants than the wild type strain.

In this study, we investigated the factors responsible for the spatiotemporal colonization of PPFM in the phyllosphere. We studied the behavior of *Methylobacterium* sp. strain OR01 at a single-cell level during the growth of red perilla, and followed its entire journey from seeds to the whole plant surface, and subsequently to the next-generation seeds. Fluorescent and electron microscopical observations elucidated the bacterial distribution and dynamic behavior in the phyllosphere. With the analyses of mutants impaired in FliC (the flagellin protein) and MptA of strain OR01, we demonstrate the importance of motility and methylotaxis in phyllosphere colonization of strain OR01 and show a novel function of methanol as a volatile messenger in the phyllosphere during symbiosis between PPFMs and the host plant.

Fluorescent single-cell analysis revealed the transmission of PPFM through plant tissue surfaces to seeds for the next generation.

Methylobacterium sp. strain OR01 expressing GFP (strain OR01-GFP) was inoculated onto seeds of red perilla and the bacterial behavior was followed by fluorescence. Three to four months after inoculation, aerial parts of the plant (the second leaf, newest leaf, petiole, stem, terminal bud, axillary bud and flower, as well as the next-generation seeds picked up from the seed bag of the flower) were harvested at various stages (Fig. 1A). The collected samples were rinsed in sterile water and spread onto a minimal medium (hypho medium) agar plate supplemented with methanol as a single carbon source. GFP-fluorescent colonies appeared on all the tested plates, confirming the presence of strain OR01-GFP on the surface of the entire red perilla plant (Fig. 1B). We also quantified the cell number of the strain OR01 expressing mCherry (strain OR01-mCherry) using flow cytometry (FCM) analysis to understand the localization of the bacteria. Similar to colony formation analysis, aerial parts of the perilla plant were harvested three to four months after strain OR01-mCherry was inoculated onto seeds. FCM analysis revealed that about 13,000 cells were present per mg of the axillary bud, while approximately 2,000 cells were present on the petiole, terminal bud and stem (Fig. 1C). Among the leaf samples, the largest number of cells was detected with new leaf samples. These results indicated that a higher number of bacteria colonize younger plant tissues such as axillary bud and

the newest leaves. We also harvested new seeds from flowers and placed them onto a hypho medium agar plate for direct observation by a transilluminator imaging system (Fig. 1D). In addition, cells of strain OR01 were isolated from the seeds placed on the agar plate for microscopic observation (Fig. 1E). We detected GFP fluorescence from the plant and bacterial samples, demonstrating that strain OR01-GFP traveled throughout the surface of plant tissues, and colonized the next-generation seeds.

PPFM preferentially resides at the base of the trichome, along the vein and around the stomata.

To investigate the bacterial distribution on plant leaves, a leaf-print assay was performed with the first true leaves. We found that strain OR01-GFP was distributed throughout both adaxial and abaxial sides of the leaves (Fig. 2A). A confocal microscopic analysis found that bacterial colonies were present particularly at the base of the trichomes (Fig. 2B left image), along the vein (central image) and around the stomata (right image). Interestingly, GFP fluorescence was detected not only around but also inside the stomata. The z-stack images found that a substantial number of strain OR01-GFP was present in the sub-stomatal cavity (Fig. 2C and Supplementary Movie 1).

To further analyze strain OR01-GFP on the leaf surface, correlative light and electron microscopy (CLEM) was performed. We found that numerous clumps were present throughout the leaf surface (Supplementary Fig. 1A). Enlarged images revealed that strain OR01-GFP cells were present around the trichome in biofilm-like structures that were about 20 μm x 20 μm long vertically and horizontally (Fig. 2D). Furthermore, CLEM captured the presence of strain OR01-GFP around the stomata (Supplementary Fig. 1B). Under higher magnification, strain OR01-GFP was detected inside the stomata (Fig. 2E), as demonstrated in Fig. 2B-C with the confocal microscope. To investigate the bacterial dynamics around the stomata, we monitored the strain OR01-GFP that existed around the stomata over time. Interestingly, the videography captured the moments of strain OR01-GFP entering the stomata (Fig. 2F and Supplementary Movie 2). Within the recorded 77 seconds, four cells of strain OR01-GFP moved into the stomata and these cells were observed to track the same path (Supplementary Movie 2). Several non-GFP-labeled cells were also detected, but they did not enter into the stomatal cavity.

FliC (flagellin)-dependent motility and bacterial distribution in the phyllosphere

Our observation of the cell entry into the stomata prompted us to speculate that bacterial distribution in the phyllosphere is affected by flagellin-dependent motility. We constructed a gene-deletion strain OR01 lacking all of the flagellin proteins, i.e., *fliC1*,

fliC2 and *fliC3*, that expressed GFP (strain Δ*fliC*-triple-GFP). Deletion of these three genes resulted in complete loss of flagella (Supplementary Fig. 2A-B) and significant loss of motility (Supplementary Fig. 2C-D and Supplementary Movie 3, 4).

We inoculated strain Δ*fliC*-triple-GFP and strain OR01-mCherry on red perilla seeds and harvested the first and second true leaves one month after cultivation. Leaf-print assay revealed that the GFP fluorescence of strain Δ*fliC*-triple-GFP was much weaker than the mCherry fluorescence of strain OR01-mCherry under both single and mixed inoculation conditions (Fig. 3A-B). FCM-based quantitative analysis counted approximately 20,000 cells of strain OR01-mCherry and 5500 cells of strain Δ*fliC*-triple-GFP per mg of perilla leaf under single inoculation conditions (Fig. 3C). Under mixed inoculation conditions, the difference between these strains became more pronounced in that the cell number of strain OR01-mCherry remained around 15000, whereas that of strain Δ*fliC*-triple-GFP was reduced to less than 300 (Fig. 3D). These results suggested that bacterial motility promoted phyllosphere colonization of strain OR01 during transmission from seeds to the phyllosphere. However, strain Δ*fliC*-triple-GFP significantly colonized the peripheral regions around the base of the trichome (Fig. 3A-B), indicating that bacterial motility is not responsible for peripheral colonization as much, but is critical for movement toward the center of the leaf surface. This observation could be explained by the assumption that bacteria do not require motility for colony formation in the leaf periphery if they can proliferate on vegetative tissue of the plant (e.g., the meristem of the growing leaf) during the entire growth period.

MtpA-dependent methylotaxis accelerates stomatal entry and colonization of PPFM to the leaf surface

Bacterial chemotaxis is driven by a signal transduction mechanism involving MCPs and Che proteins and the directional movement controlled by the flagellin protein FliC (Fig. 4A). To further investigate the involvement of chemotaxis in phyllosphere colonization, we focused on methylotaxis. We disrupted *mtpA* (homologous to methylotaxis protein A found in *M. aquaticum* strain 22A) (MamtpA, identity: 49%, similarity: 63%) in the genome of strain OR01 (Supplementary Fig. 3A-B). Stereo microscopic and FCM analyses using the strain Δ*mtpA* expressing GFP (strain Δ*mtpA*-GFP) revealed that deletion of the *mtpA* gene led to a significant reduction in methylotaxis of strain OR01 without disrupting chemotaxis to succinate (Supplementary Fig. 4A-B), indicating that MtpA is a major chemoreceptor for methanol in strain OR01. In a similar manner to strain OR01-GFP, we inoculated strain Δ*mtpA*-GFP onto the abaxial surface and examined the stomatal entry of the mutant strain. Microscopic analysis demonstrated that the cell

number of strain Δ*mtpA*-GFP present in the stomata was significantly lesser than that of strain OR01-GFP (Fig. 4B). A similar analysis was performed with strain Δ*fliC*-triple-GFP (Fig. 4B), which revealed that the lack of FliC proteins resulted in further reduction in the number cells detected compared to that in strain Δ*mtpA*-GFP. Quantitative analysis revealed that 65% of the total area of open stomata was covered by GFP fluorescence of strain OR01-GFP, whereas only 17% and 0.1% were covered by GFP fluorescence of strain Δ*mtpA*-GFP and strain Δ*fliC*-triple-GFP, respectively (Fig. 4C).
In addition, at least one cell of strain OR01-GFP was observed in more than 95% of the stomata, whereas cells of strain Δ*mtpA*-GFP were present in approximately 52% of the stomata and those of strain Δ*fliC*-triple-GFP were not detected (Fig. 4D), demonstrating that MtpA is responsible for strain OR01 to enter into the stomatal cavity.

Subsequently, we investigated the physiological significance of MtpA-dependent methylotaxis in bacterial colonization in the phyllosphere of red perilla. After sterilization, red perilla seeds were inoculated with either strain OR01-mCherry or strain Δ*mtpA*-GFP. Two months after plant growth under single inoculation conditions with bacterial cells, we performed the leaf-print assay and found a significant reduction in the fluorescence of GFP from strain Δ*mtpA*-GFP when compared with strain OR01-mCherry (Fig. 4E). We also detected a higher proportion of strain Δ*mtpA*-GFP present in the peripheral part of the leaf compared to strain OR01-mCherry. Quantitative analysis by FCM revealed that an average of 20,000 cells per mg of the plant sample was detected from the leaf inoculated with strain OR01-mCherry, whereas only about 4,000 cells of strain Δ*mtpA*-GFP were counted from the collected leaf sample (Fig. 4F), suggesting that methylotaxis plays a critical role in the colonization of strain OR01 in the phyllosphere.

Although the *mtpA* deletion led to a significant reduction in the bacterial entry into the stomatal cavity and colonization on the leaf surface, its impact was not as large as the complete loss of flagellin (Fig. 4B-D). Next, the chemotactic response to red perilla extract was investigated by fluorescence stereo microscopy and FCM. Strain OR01-mCherry and strain Δ*mtpA*-GFP showed a similar chemotaxis activity to the red perilla extract (Supplementary Fig. 4C-D), suggesting that some attractants other than methanol present in perilla extract attract strain OR01, eventually contributing to their stomatal entry and colonization.

To investigate the intracellular localization of MtpA in strain OR01, we constructed the Δ*mtpA* strain expressing GFP-MtpA fusion protein (strain Δ*mtpA*-GFP-MtpA). The functionality of the fusion protein was confirmed by complementation experiment of methylotaxis, using strain OR01, strain Δ*mtpA* and strain Δ*mtpA*-GFP-MtpA (Supplementary Fig. 4E). During cultivation on methanol, GFP-MtpA signal was found

to form foci and localize mainly to the poles of cells (Fig. 4G), suggesting that MtpA in strain OR01 form the chemotaxis sensory array at the cell pole together with Che proteins, in a manner similar to that previously demonstrated in other MCPs[18]. Subsequently, we inoculated strain Δ*mtpA*-GFP-MtpA onto the leaf surface of red perilla and found that GFP-MtpA localized at the cell pole (Fig. 4H). These results suggested that MtpA is responsible for methylotaxis in the phyllosphere.

The predominant colonization of strain OR01 on red perilla is attributed to its high methylotaxis activity

Strain OR01 is predominant in the phyllosphere of red perilla[8]. Next, we set out to analyze the reason for this predominance by performing a competitive colonization analysis of mCherry-expressing strain OR01 (strain OR01-mCherry-g) with mVenus-expressing *M. aquaticum* strain 22A (strain 22A-mVenus-g). With a single inoculum of each strain, we found that strain OR01-mCherry-g and strain 22A-mVenus-g were distributed throughout the leaf surface both on the adaxial and abaxial sides (Fig. 5A). However, inoculation conditions in a mixed inoculum led to a substantial decrease in the fluorescence of mVenus of strain 22A-mVenus-g cells in comparison with that of strain OR01-mCherry-g on both sides of the leaf surface (Fig. 5B). mCherry fluorescence in OR01-mCherry-g was distributed throughout the leaf surface, while mVenus in 22A-mVenus-g was scattered as dots and did not spread uniformly. To quantify the number of cells, the first, second, and third true leaves were collected regularly for FCM analysis. Under inoculation conditions in a single inoculum, ca. 5,000 to 20,000 cells of strain OR01-mCherry-g and ca. 2,500 to 12,000 cells of strain 22A-mVenus-g were detected per mg perilla leaf, and there was no statistical difference between these two strains (Fig. 5C). With mixed inoculum of both strains, we found a significant difference in that the cell number of strain OR01-mCherry-g was ca. 5,000 to 25,000, whereas that of strain 22A-mVenus-g was 300 to 3,000 (Fig. 5D). These results indicated that strain OR01 is more competitive than strain 22A in colonization on red perilla.

Finally, we explored the characteristics that allowed strain OR01 to be competitive on red perilla by a capillary chemotaxis assay. Analysis by stereo microscopy revealed that methylotaxis activity of strain OR01-mCherry-g was much higher than that of strain 22A-mVenus-g (Fig. 5E), which became more significant under inoculation conditions in a mixed inoculum (Fig. 5F). FCM analysis quantified that the cell number of strain OR01-mCherry-g was approximately 10,000, whereas that of strain 22A-mVenus-g was 200 with a single inoculum (Fig. 5G). With a mixed inoculum, the cell number of strain OR01-mCherry-g was 10,000, whereas that of strain 22A-mVenus-g was reduced to 100, which

was consistent with the analysis by stereo microscopy (Fig. 5H). To explore the sensitivity of strain OR01 to methanol further, we performed a capillary chemotaxis assay supplemented with 0.00001% and 0% methanol. We found that strain OR01 migrated into a capillary containing just 0.00001% methanol, while it showed no movement towards a capillary lacking methanol, demonstrating the remarkable sensitivity of strain OR01 to methanol (Supplementary Fig. 5).

In addition, we also performed the capillary chemotaxis assay with the red perilla extract. Analysis of these two strains by stereo microscopy revealed that their chemotactic response was similar to each other under inoculation conditions in a single inoculum (Fig. 5I), whereas inoculation conditions in a mixed inoculum resulted in a much higher chemotaxis of strain 22A-mVenus-g to red perilla extract than that of strain OR01-mCherry-g (Fig. 5J). FCM analysis quantified with a single inoculum showed that the numbers of cells per μL of red perilla extract were around 1,000 and 1,300 in strain OR01-mCherry-g and strain 22A-mVenus-g with no statistical difference between these strains (Fig. 5K). With a mixed inoculum, the cell number of strain OR01-mCherry-g was 2,000, whereas that of strain 22A-mVenus-g was reduced to 300, also consistent with the analysis by stereo microscopy (Fig. 5L). These results suggest that methylotaxis activity of strain OR01 significantly enhanced its competitiveness on red perilla compared to other strains on perilla leaves.

Discussion

This study demonstrates that methanol-sensing MtpA, which drives methylotaxis, determines the spatiotemporal colonization of *Methylobacterium* sp. strain OR01 in the phyllosphere of its natural host, the red perilla plant. During its transmission, strain OR01 was present in the entire leaf surface with a preference to sites around the periphery, vein, trichome and stomata of the leaf surface. Strain OR01 entered the sub-stomatal cavity attracted by methanol and this behavior was attributed to MtpA-driven methylotaxis and FliC-dependent motility. Furthermore, their high methylotaxis activity contributed to the competitiveness of strain OR01 on red perilla (Fig. 6).

Of particular interest is the MtpA-dependent entry of strain OR01 into the stomata (Fig. 2F and Supplementary Movie 2). Previously, we developed a methanol cell sensor and directly determined the local methanol concentration on the leaf surface of *Arabidopsis thaliana* to be 0–0.21% (0–64 mM) with a periodic methanol oscillation, i.e. high in the dark and low in the light period[14], which might be directly linked to the hydrolyzation of pectin in the plant cell wall. We confirmed the high methanol-sensing ability of strain OR01 using a capillary assay, which showed that strain OR01 entered the capillary supplemented with 0.00001% methanol whereas it did not move to the capillary without methanol (Supplementary Fig. 5). The methanol sensing machinery comprising Wsc1 and Wsc3 in the yeast *Komagataella phaffii* senses methanol concentration in the range between 0.005 and 1%. In comparing the bacterial and yeast methanol-sensing machineries, MtpA in strain OR01 is 500-fold more sensitive than the yeast methanol sensor Wsc, suggesting that methanol not only serves as a carbon source for strain OR01, but also functions as a volatile messenger for communication with the host plant.

One possible benefit for the host plant to attract PPFMs to the stomatal cavity is the *in-situ* oxidation of methanol to CO_2, which is directly fixed by plants through photosynthesis (Fig. 6). A previous study with ^{13}C-methanol labeling and liquid chromatography-mass spectrometry analyses suggested that methanol present on the leaf surface was primarily oxidized to CO_2 for energy generation in PPFM, although a portion of the methanol entered into the methanol assimilation pathway[19]. Another benefit of bacterial presence in the stomatal cavity for plants may be the increased protection from pathogenic invasion. *Pseudomonas syringae*, a widely studied plant pathogen, is known to enter the stomatal cavity during infection[20-24]. Therefore, attracted by methanol, PPFMs may move to the stomatal cavity and occupy the colonization place prior to pathogens. Other than the stomatal cavity, invasion of pathogens to the host cells yielded methanol by secreted pectinases[25], which might attract PPFM to the invasion site.

Previously, we reported that many PPFMs isolated from plant samples require B vitamins for growth on minimal media, e.g., pantothenate (vitamin B_5)[26]. It may be advantageous for PPFMs to colonize sites like glandular trichome to acquire nutrients other than methanol that are necessary for bacterial growth[27].

Deletion of the *mtpA* gene responsible for methylotaxis and *fliC* genes required for motility led to a significant decrease in the number of cells entering the stomata and colonizing red perilla leaves (Fig. 4). The role of chemotaxis and/or motility in bacterial colonization has been studied extensively with rhizosphere bacteria, and previous studies have revealed their significance in competitive root surface colonization and establishment of a successful symbiosis[28-31]. In addition to colonization and symbiosis, transmission is also reported to be supported by bacterial movement[32]. The physiological role of chemotaxis has also been investigated using pathogenic bacteria. A previous report has identified AreA and AreB, the genes responsible for chemotaxis in *P. syringae*, as contributing to the pathogenic invasion of the host plant[33]. Another study has found that chemotaxis to nitrate and nitrite contributes to the colonization of the pathogen *Dickeya dadantii* on its host plant[34]. However, insights from these studies have been limited to the rhizosphere, in particular to nitrogen fixation bacteria and the loci for pathogenic invasion. Our study has shed light on bacterial chemotaxis and motility of phyllosphere microorganisms by demonstrating their crucial role in colonizing the host plant through its entire life cycle, rather than being confined to a specific part or developmental stage of the plant. To our knowledge, this is also the first report to show methanol as a compound that attracts phyllosphere bacteria to enter stomatal pores.

Methods

Bacterial strains and culture conditions

The bacterial strains used in this study are listed in Supplementary Table 1. *Methylobacterium* sp. strain OR01 and *M. aquaticum* strain 22A were grown at 28°C in the hypho minimal medium (Supplementary Table 2)[29] containing one of the carbon sources described below and all of the B-group vitamins (Vitamin mix). Carbon sources were 0.5% or 0.05% (v/v) methanol, 0.5% or 0.05% (w/v) disodium succinate or 0.4% (w/v) extract from red perilla leaves. The antibiotic kanamycin (Km, 20 μg/mL) was added as needed. *Escherichia coli* HST08 premium competent cells (TaKaRa) were used for gene cloning. *E. coli* was grown at 37°C on LB medium (1% Bacto tryptone, 0.5% Bacto yeast extract and 0.5% NaCl) in the presence of ampicillin (50 μg/mL) or kanamycin (20 μg/mL). The nucleotide sequences of *fliC1*, *fliC2*, *fliC3*, *mtpA* and *mxaF* were deposited in the DDBJ/EMBL/GenBank under accession numbers LC833873, LC833874, LC833875, LC833876 and LC833877, respectively.

Construction of plasmids

The plasmids used in this study are listed in Supplementary Table 3, and the oligonucleotide primers are listed in Supplementary Table 4. The plasmid vectors pBluescript II SK(+) (Stratagene Inc), pDCG-1[35], pMO149[36], pAT02-V[17], pCM80-Km[37], pCM1682[13] and pK18 mobsacB[35] were used in previous studies.

The vector pBS-P_{mxaF} was constructed as follows: The promoter region of the gene *mxaF* was PCR-amplified by using the genomic DNA of *Methylobacterium* sp. strain OR01 with a primer pair PmxaF-Fw-KpnI/PmxaF-Rv-HindIII. After digestion with *Kpn*I and *Hind*III, the DNA fragment was ligated with linearized pBluescript II SK(+) with the same set of restriction enzymes. Subsequently, the primer pairs GFP-Fw-HindIII/GFP-Rv-PstI and mCherry-Fw-HindIII/mCherry-Rv-BamHI were used to amplify the 0.7-kb *GFP* and *mCherry* genes with pDCG-1 and pMO149 as templates, respectively. The PCR products with *GFP* and *mCherry* sequences were ligated into the linearized pBS-PmxaF by restriction enzyme sets, *Hind*III-*Pst*I and *Hind*III-*Bam*HI, respectively, resulting in the pBS-PmxaF-GFP and pBS-PmxaF-mCherry vectors.

The pCM802-based vectors were constructed from a plasmid vector pCM80-Km[37]

given by Dr Toshiaki Fukui. The *mxaF* promoter region of *M. extorquens* strain AM1 was removed using a primer set pCM80km-Re1800/pCM80km-Fw2471 by inverse PCR with pCM80-Km as a template, followed by self-ligation, yielding pCM802-Km. The vectors pCM802-Km and P_{mxaF}-GFP were digested by *Kpn*I and *Pst*I and ligated to each other, resulting in the plasmid pCM802-GFP. Similarly, the vectors pCM802-Km and P_{mxaF}-mCherry were cut by *Kpn*I and *Sph*I, and these DNA fragments were ligated to obtain the plasmid pCM802-mCherry. The vector pCM802-GFP-mtpA was constructed as follows: The promoter and ORF regions of *mtpA* were PCR-amplified using primer pairs NB_PmtpA_Fw/NB_PmtpA+GFP_Rv and NB_PmtpA+GFP_Fw/NB_GFP+mtpA_Rv with the genomic DNA of strain OR01 as templates. The *GFP* coding sequence was amplified by PCR using a primer pair NB_GFP+mtpA_Fw/NB_mtpA_Rv with pCM802-GFP as a template. These two DNA fragments were cloned into the *Bam*HI and *Sac*I sites of pCM802-Km by NEbuilder cloning kit (New England Biolabs), resulting in the vector pCM802-GFP-mtpA. These pCM802-based vectors were used as vectors for expression in plasmids.

The plasmid vectors pCM1684 and pCM1685 for genome insertion into strains OR01 and 22A, respectively, were constructed as follows: pCM1684 was constructed by ligating pCM1682-derived sequences with a strain OR01 chromosome region at 404241 locus where no gene was assigned, and further with P_{mxaF}-mCherry sequence amplified from pCM802-P_{mxaF}-mCherry. Similarly, pCM1685 was constructed by ligating pCM1682-derived sequences with a strain 22A chromosome region at 1718735 locus where no gene was assigned, and further with P_{mxaF}-Venus sequence amplified from pAT02-Venus. These ligation processes were achieved by an NEbuilder cloning kit, resulting in the vector pCM802-GFP-mtpA.

The plasmid vectors for precise in-frame deletion of *mtpA*, *fliC1*, *fliC2* and *fliC3* genes were constructed as follows: pK18mobsacB carrying a positive selection marker (Km^r gene) and a counter-selectable marker (suicide gene *sacB*) was used for constructing all the pK18-based plasmid vectors for gene disruption, as previously described[30,31]. Subsequently, the disruption vector pK18 ΔfliC1 was constructed as follows: The *fliC1* and the homologous fragment flanking *fliC1* were PCR-amplified using a primer pair fliC1_up_Fw/ fliC1_down_Rv with the genomic DNA of strain OR01 as a template. The

DNA fragment and pK18mobsacB, digested by restriction enzymes *Sal*I and *Sph*I, were ligated to each other, resulting in the plasmid pK18 fliC1. The *fliC1* ORF region was removed using a primer set Inv_fliC1_Fw1/ Inv_fliC1_Rv by inverse PCR with pK18 fliC1 as a template, followed by a self-ligation, yielding the vector pK18 ΔfliC1. The disruption vectors pK18 ΔfliC2 and pK18 ΔmtpA were constructed in a similar manner. The ORF, upstream and downstream region of *fliC2* and *mtpA* were PCR-amplified using primer pairs fliC2_up_Fw/ fliC2_down_Rv and mtpA_up_Fw/mtpA_down_Rv, respectively, with the genomic DNA of strain OR01 as a template. The DNA fragments and pK18mobsacB, digested by restriction enzymes *Sal*I and *Sph*I, were ligated to each other, resulting in the plasmid pK18 fliC2 and pK18 ΔmtpA. The disruption vector pK18 ΔfliC3 was constructed as follows: the homologous fragments flanking *fliC3* were amplified by PCR using primer pairs fliC3_up_Fw/ fliC3_up_Rv and fliC3_down_Fw/ fliC3_down_Rv with the genomic DNA of strain OR01 as a template. These fragments were cloned into the *Sal*I and *Sph*I sites of pK18mobsacB by an NEbuilder cloning kit.

Transformation of DNA to *Methylobacterium* sp. OR01 and *M. aquaticum* strain 22A

Cells were grown for 48 hours and 500 μL of them were centrifuged at 15,000 rpm for 1 minute. To prepare for competent cells of *Methylobacterium* sp. OR01, harvested cells were washed with sterilized water and then resuspended in 50 μL of sterilized water. For *M. aquaticum* strain 22A, collected cells were washed with 10% glycerol and then resuspended in 50 μL of sterilized water containing 10% glycerol and 30% PEG. Competent cells were mixed with 1 μL of DNA and transferred to 1 mm gap cuvette (Bio-Rad). The DNA was introduced to the cells by electroporation at 1.8–2 kV, 25 μF, 200 Ω (GenePulser Xcell™, Bio-Rad). The entire electroporated suspension was inoculated into 500 μL Nutrient Broth (Difco™) medium and cultured for 3 hours at 28°C. These cells were plated on the hypho medium plates containing 0.5% succinate and vitamin mix and incubated at 28°C for 3–5 days. For obtaining gene knockout strains, the grown colonies were streaked on R2A agar medium containing 10% sucrose, 0.5% succinate and 1% vitamin mix. After culturing at 28°C for about 5 days, mutant strains were selected by colony PCR.

Cultivation of red perilla

Red perilla was grown in a plastic cup about 20 cm high with vermiculite and a ventilated seal or in a plastic dish about 4 cm high with Hoagland agar as described previously[8]. The plants were placed in the NK Biotron LH-220 (Nippon Medical and Chemical Instruments, Osaka, Japan). The system was operated at 25°C, 65% humidity under a 15-h light 9-h dark cycle. Plants cultivated on agar media developed in the same way as plants grown in plastic cups containing vermiculite for the first 2 weeks. Thereafter, a dwarf phenotype was observed, but they appeared healthy otherwise.

Measurement of cell populations of PPFMs on red perilla

Cells of the strain OR01 and strain 22A were grown on the hypho medium containing 0.5% methanol and vitamin mix at 28°C for 2 days. After collection, cells were washed with sterilized water and suspended in sterilized water to obtain a suspension with an OD_{600} of 0.1. Red perilla seeds were treated with 70% ethanol for 1 minute and with 1% (v/v) antiformin (containing 0.3% v/v Tween 20) for 5 minutes, followed by washing with sterilized water 5 times. They were soaked in 1 mL of the single or mixed (wild type strain and each mutant strain) cell suspension for 3 hours with gentle shaking at 5 rpm using a Rotator RT-5 (Taitec, Saitama, Japan) at 28°C. The seeds incubated with *Methylobacterium* sp. OR01 were sown onto Hoagland agar in a plant culture dish (100×40 mm) or vermiculite for growth in the chamber. For the collection of PPFMs from red perilla, the leaves were cut and placed in a 1.5 mL tube, weighed, and then,100 μL of PBS was added per 10 mg of leaf and vortexed for 15 minutes. 20 μL of this collection sample was mixed with 20 μL of BD™ Liquid counting Beads (BD Biosciences) and 200 μL of PBS and the total volume was used for FCM, which was performed as previously described[17].

Colony formation analysis

After sterilization, as previously described[8], red perilla seeds were suspended in cells of strain OR01-GFP for 3 hours and sown onto Hoagland agar or vermiculite. Three to four months after aseptic growth, aerial parts of the plant were harvested. The collected samples were rinsed, suspended in sterile water and spread onto the hypho medium agar

plate containing 0.5% methanol with kanamycin (20 μg/mL) as needed. To visualize colonies, the FAS-Digi imaging system (NIPPON Genetics) was employed.

Microscopic observations

Fluorescence stereo microscope SZX16 (OLYMPUS), confocal microscopes Zeiss LSM510 META/Axiovert 200 (Olympus), FV3000 (Olympus), and FV4000 (Olympus), BX51 (Olympus), SU8220 (Hitachi High-Tech) and IX73 inverted microscope (Olympus) were used in this study. The images were captured and processed using Olympus cellSens software. Details of these microscopes are as follows:

Fluorescence stereo microscope SZX16 is equipped with a digital charge-coupled device camera (Olympus DP80), a GFP filter (Olympus SZX2-FGFPHQ) and an RFP filter (Olympus SZX2-FRFP2). SZX16 was used for Fig. 2a, 3c, 3d, 4d, 5a, 5b, 5e, 5f, 5i, 5j, and Supplementary Fig. 4a and 4c.

Zeiss LSM510 META/Axiovert 200 is equipped with a Plan Fluor 100×/1.45 NA oil objective. GFP and mVenus fluorescence were obtained with a multiline 488 argon laser and a 505–550 nm filter for emission. An HFT 405/514 beam splitter was used as a connecting filter. Zeiss LSM510 META/Axiovert 200 was used for Fig. 1c, 2b, 2c, 2f, and Supplementary Movie 1 and 2.

FV3000 is equipped with six solid-state diode lasers (405 nm, 445 nm, 488 nm, 514 nm, 561 nm, and 640 nm), whereas FV4000 comes with ten laser lines ranging from 405 nm to 785 nm. They use Olympus objectives including PLAPON 60x (1.42 NA, oil-dipped) and UPLSAPO 100x (1.35 NA, Si oil-dipped). For image detection, the FV3000 is equipped with high-sensitivity GaAsP detectors, enabling the detection of faint fluorescence signals with high signal-to-noise ratios. FV4000 uses the SilVIR detector, which combines a silicon photomultiplier (SiPM) with advanced signal processing. FV3000 was used for Fig. 4a and 4f, while FV4000 was used for Fig. 4g.

BX51 is equipped with a digital charge-coupled device camera (Olympus DP71). It uses Olympus objectives including UPlanSApo 4x/0.16, UPlanSApo 10x/0.40, UPlanSApo 20x/0.75 and UPlanSApo x40/0.95. The mirror unit for GFP is U-MNIBA3 (Olympus). BX51 was used for Fig. 2d, 2e and Supplementary Fig. 1.

SU8220 was used at 15 or 20 kV accelerating voltage. The scanning mode for high magnification is SE(UL). The electron microscope was used for Fig. 2d, 2e and Supplementary Fig. 1.

IX73 inverted microscope is equipped with a lens UPLAPO OI3 100x / 1.35 and flagellar length was measured by CellSens using the data taken as differential interference contrast (DIC) images. The microscope was used for Supplementary Fig. 2a, 2c, 2d, 4a, 4c and Supplementary Movie 3 and 4.

Capillary chemotaxis assay

Chemotaxis was evaluated using capillaries and a glass slide with a hole[27]. Two capillaries were placed on each side of the hole as spacers between the cover glass and the glass slide. Hypho medium supplemented with a carbon source at a concentration of 0.05%, as necessary, vitamin mix and appropriate antibiotics were sucked into a new capillary. Then, one hole was closed with nail polish and placed on the hole glass slide, followed by a cover glass set over the capillary. For red perilla extract, 1 mL of hypho medium was added to 4.1 mg of red perilla leaves and mashed with a mortar and pestle. Then, the obtained extracts were filtered for experiments. 200 μL of bacterial suspension of OD_{600} at 0.01 was applied to the hole portion of the glass slide with a hole and incubated at 28°C for 3 hours. After culturing, the cells in the capillary were observed with an SZX16 fluorescence stereo microscope (OLYMPUS). The number of cells in the capillary was examined as previously described[17].

Microscopic analysis of cell entry to a single pore of the stomata

Leaves were placed statically overnight on a bacterial solution containing hypo medium with no carbon source. The bacterial solution was prepared at OD_{600} 0.1. The leaves were then observed by confocal microscopes FV3000 (Olympus) and FV4000 (Olympus) for quantitative analysis.

Leaf-print assay

The harvested leaves of red perilla were cut and placed directly on the hypho medium

agar plate containing 0.5% methanol or 0.5% succinate with the addition of kanamycin (20 μg/mL), as needed. Then, the leaf was gently pressed to the medium using a spreading stick and incubated at 28°C for 3–4 days. After the culture, microbial distribution was observed by the SZX16 fluorescence stereo microscope (OLYMPUS).

CLEM analysis

Red perilla seeds were sterilized and treated with the cell suspension of strain OR01-GFP. They were sown onto Hoagland agar in a plant culture dish for growth in a chamber. One month after aseptic growth, aerial parts of the plant were harvested. Samples were fixed with a solution of 2% paraformaldehyde, 2.5% glutaraldehyde, 0.1 M phosphate buffer, pH 7.4 for 30 minutes at room temperature. Subsequently, these samples were used for CLEM analysis. After fixation, these samples were suspended and stored in phosphate-buffered saline. Subsequently, the samples were mounted on a glass slide and fluorescent and Bright-field images were acquired with BX51. After washing in 0.1 M phosphate buffer (pH7.4) three times, the samples were frozen in liquid nitrogen for 2 minutes and freeze-dried overnight (Yamato Scientific Co., ltd. DC-56A). Then, the samples were mounted on SEM stubs using double-sided carbon tape and coated with 7 nm osmium in an HPC-1SW coater (Shinku Device). A scanning electron microscope (Hitachi High-Tech SU8220) was used for imaging according to the manufacturer's protocol. After image acquisition, images were merged using Photoshop 2024 (Adobe).

Flagella visualization

Living cells were stained for flagella visualization using the staining solution by Ryu[38] and a method similar to Heimbrook and colleagues[4]. Visualized flagella were investigated with an IX73 inverted microscope (Olympus) and the length of flagella was analyzed by cellSens.

Acknowledgments

This paper was supported in part by JSPS KAKENHI, Grant Numbers 19H02870 to Y.S. and 19K22307, 22K19133, 24H02120 to H.Y, and by GteX Program Japan Grant Number JPMJGX23B4 to K.S., and the Joint Usage/Research Center, Institute of Plant Science and Resources, Okayama University to A.T. We thank Dr Toshiaki Fukui and Dr Izumi

Orita for gifting us the plasmid vector pCM80-Km.

Author contribution

S.K., K.S., H.Y., A.T. and Y.S. conceived the study. S.K., K. Kaji, K. Kawabata, N.T. and A.T. conducted the investigations. S.K., K.S., K. Kaji, K. Kawabata, H.Y. and Y.S. analyzed the data. K.S. wrote the original manuscript with inputs from S.K., K. Kaji, K. Kawabata, and N.T. A.T., H.Y. and Y.S. reviewed and edited the manuscript. K.S., A.T., H.Y. and Y.S. acquired the funding.

Competing interests

The authors declare no competing interests.

Supplementary information

Supplementary Figures 1-5, Tables 1-4, Movies 1-4, legends for Supplementary Figures and references.

References

1. Delmotte, N. *et al.* Community proteogenomics reveals insights into the physiology of phyllosphere bacteria. *Proc. Natl Acad. Sci. USA* **106**, 16428-16433 (2009).
2. Senthilkumar, M., Madhaiyan, M., Sundaram, S. & Kannaiyan, S. Intercellular colonization and growth promoting effects of *Methylobacterium* sp. with plant-growth regulators on rice (Oryza sativa L. Cv CO-43). *Microbiol. Res.* **164**, 92-104 (2009).
3. Hornschuh, M., Grotha, R. & Kutschera, U. Moss-associated methylobacteria as phytosymbionts: an experimental study. *Naturwissenschaften* **93**, 480-486 (2006).
4. Madhaiyan, M., Poonguzhali, S., Ryu, J. & Sa, T. Regulation of ethylene levels in canola (Brassica campestris) by 1-aminocyclopropane-1-carboxylate deaminase-containing *Methylobacterium fujisawaense*. *Planta* **224**, 268-278 (2006).
5. Koenig, R.L., Morris, R.O. & Polacco, J.C. tRNA is the source of low-level trans-zeatin production in *Methylobacterium* spp. *J. Bacteriol.* **184**, 1832-1842 (2002).
6. Ardanov, P., Sessitsch, A., Häggman, H., Kozyrovska, N. & Pirttilä, A.M. *Methylobacterium*-induced endophyte community changes correspond with protection of plants against pathogen attack. *PLoS One* **7**, e46802 (2012).
7. Yurimoto, H. *et al.* Methanol bioeconomy: promotion of rice crop yield in paddy fields with microbial cells prepared from natural gas-derived C(1) compound. *Microb. Biotechnol.* **14**, 1385-1396 (2021).
8. Mizuno, M., Yurimoto, H., Iguchi, H., Tani, A. & Sakai, Y. Dominant colonization and inheritance of *Methylobacterium* sp. strain OR01 on perilla plants. *Biosci. Biotechnol. Biochem.* **77**, 1533-1538 (2013).
9. Mercier, J. & Lindow, S.E. Role of leaf surface sugars in colonization of plants by bacterial epiphytes. *Appl. Environ. Microbiol.* **66**, 369-374 (2000).
10. Dorokhov, Y.L., Sheshukova, E.V. & Komarova, T.V. Methanol in plant life. *Front Plant Sci.* **9**, 1623 (2018).
11. Ochsner, A.M. *et al.* Use of rare-earth elements in the phyllosphere colonizer *Methylobacterium extorquens* PA1. *Mol. Microbiol.* **111**, 1152-1166 (2019).
12. Vorholt, J.A. Microbial life in the phyllosphere. *Nat. Rev. Microbiol.* **10**, 828-840 (2012).
13. Iguchi, H. *et al.* KaiC family proteins integratively control temperature-dependent UV resistance in *Methylobacterium extorquens* AM1. *Environ. Microbiol. Rep.* **10**, 634-643 (2018).
14. Kawaguchi, K., Yurimoto, H., Oku, M. & Sakai, Y. Yeast methylotrophy and

autophagy in a methanol-oscillating environment on growing *Arabidopsis thaliana* leaves. *PLoS One* **6**, e25257 (2011).

15. Hazelbauer, G.L., Falke, J.J. & Parkinson, J.S. Bacterial chemoreceptors: high-performance signaling in networked arrays. *Trends Biochem. Sci.* **33**, 9-19 (2008).
16. Parkinson, J.S., Hazelbauer, G.L. & Falke, J.J. Signaling and sensory adaptation in *Escherichia coli* chemoreceptors: 2015 update. *Trends Microbiol.* **23**, 257-266 (2015).
17. Tani, A. *et al.* Metabolism-linked methylotaxis sensors responsible for plant colonization in *Methylobacterium aquaticum* strain 22A. *Front. Microbiol.* **14** (2023).
18. Briegel, A. *et al.* Universal architecture of bacterial chemoreceptor arrays. *Proc. Natl Acad. Sci. USA* **106**, 17181-17186 (2009).
19. Peyraud, R., Kiefer, P., Christen, P., Portais, J.C. & Vorholt, J.A. Co-consumption of methanol and succinate by *Methylobacterium extorquens* AM1. *PLoS One* **7**, e48271 (2012).
20. Monier, J.M. & Lindow, S.E. Frequency, size, and localization of bacterial aggregates on bean leaf surfaces. *Appl. Environ. Microbiol.* **70**, 346-355 (2004).
21. Hirano, S.S. & Upper, C.D. Bacteria in the leaf ecosystem with emphasis on *Pseudomonas syringae*-a pathogen, ice nucleus, and epiphyte. *Microbiol. Mol. Biol. Rev.* **64**, 624-653 (2000).
22. Mansvelt, E.L. & Hattingh, M.J. Scanning electron microscopy of colonization of pear leaves by *Pseudomonas syringae* pv. *syringae*. *Canad. J. Bot.* **65**, 2517-2522 (1987).
23. Roos, I.M.M. & Hattingh, M.J. Scanning electron microscopy of *Pseudomonas syringae* pv, morsprunorum on sweet cherry leaves. *J. Phytopathol.* **108**, 18-25 (1983).
24. Timmer, L.W., Marois, J.J. & Achor, D. Growth and survival of xanthomonas under conditions nonconducive to disease development. *J. Phytopathol.* **77**, 1341-1345 (1987).
25. Komarova, T.V., Sheshukova, E.V. & Dorokhov, Y.L. Cell wall methanol as a signal in plant immunity. *Front. Plant Sci.* **5**, 101 (2014).
26. Yoshida, Y., Iguchi, H., Sakai, Y. & Yurimoto, H. Pantothenate auxotrophy of *Methylobacterium* spp. isolated from living plants. *Biosci. Biotechnol. Biochem.* **83**, 569-577 (2019).
27. Tissier, A., Morgan, J.A. & Dudareva, N. Plant Volatiles: Going 'in' but not 'out' of trichome cavities. *Trends Plant Sci.* **22**, 930-938 (2017).

28. Catlow, H.Y., Glenn, A.R. & Dilworth, M.J. Does rhizobial motility affect its ability to colonize along the legume root? *Soil Biol. Biochem.* **22**, 573-575 (1990).
29. Yost, C.K., Rochepeau, P. & Hynes, M.F. *Rhizobium leguminosarum* contains a group of genes that appear to code for methyl-accepting chemotaxis proteins. *Microbiology (Reading)* **144 (Pt 7)**, 1945-1956 (1998).
30. Miller, L.D., Yost, C.K., Hynes, M.F. & Alexandre, G. The major chemotaxis gene cluster of *Rhizobium leguminosarum* bv. viciae is essential for competitive nodulation. *Mol. Microbiol.* **63**, 348-362 (2007).
31. Scharf, B.E., Hynes, M.F. & Alexandre, G.M. Chemotaxis signaling systems in model beneficial plant-bacteria associations. *Plant Mol. Biol.* **90**, 549-559 (2016).
32. Madsen, E.L. & Alexander, M. Transport of Rhizobium and Pseudomonas through Soil. *Soil Sci. Soc. Am. J.* **46**, 557-560 (1982).
33. Ichinose, Y. *et al.* Requirement of chemotaxis and aerotaxis in host tobacco infection by *Pseudomonas syringae* pv. tabaci 6605. *Physiol. Mol. Plant Pathol.* **124**, 101970 (2023).
34. Gálvez-Roldán, C. *et al.* A nitrate-sensing domain-containing chemoreceptor is required for successful entry and virulence of *Dickeya dadantii* 3937 in potato plants. *Phytopathol.* **113**, 390-399 (2022).
35. Iguchi, H., Sato, I., Yurimoto, H. & Sakai, Y. Stress resistance and C1 metabolism involved in plant colonization of a methanotroph *Methylosinus* sp. B4S. *Arch. Microbiol.* **195**, 717-726 (2013).
36. Maeda, Y., Oku, M. & Sakai, Y. A defect of the vacuolar putative lipase Atg15 accelerates degradation of lipid droplets through lipolysis. *Autophagy* **11**, 1247-1258 (2015).
37. Orita, I., Nishikawa, K., Nakamura, S. & Fukui, T. Biosynthesis of polyhydroxyalkanoate copolymers from methanol by *Methylobacterium extorquens* AM1 and the engineered strains under cobalt-deficient conditions. *Appl. Microbiol. Biotechnol.* **98**, 3715-3725 (2014).
38. Ryu, E. A Simple method of staining bacterial flagella. *Kitasato Arch. Exp. Med.* **14**:218-219 (1937).

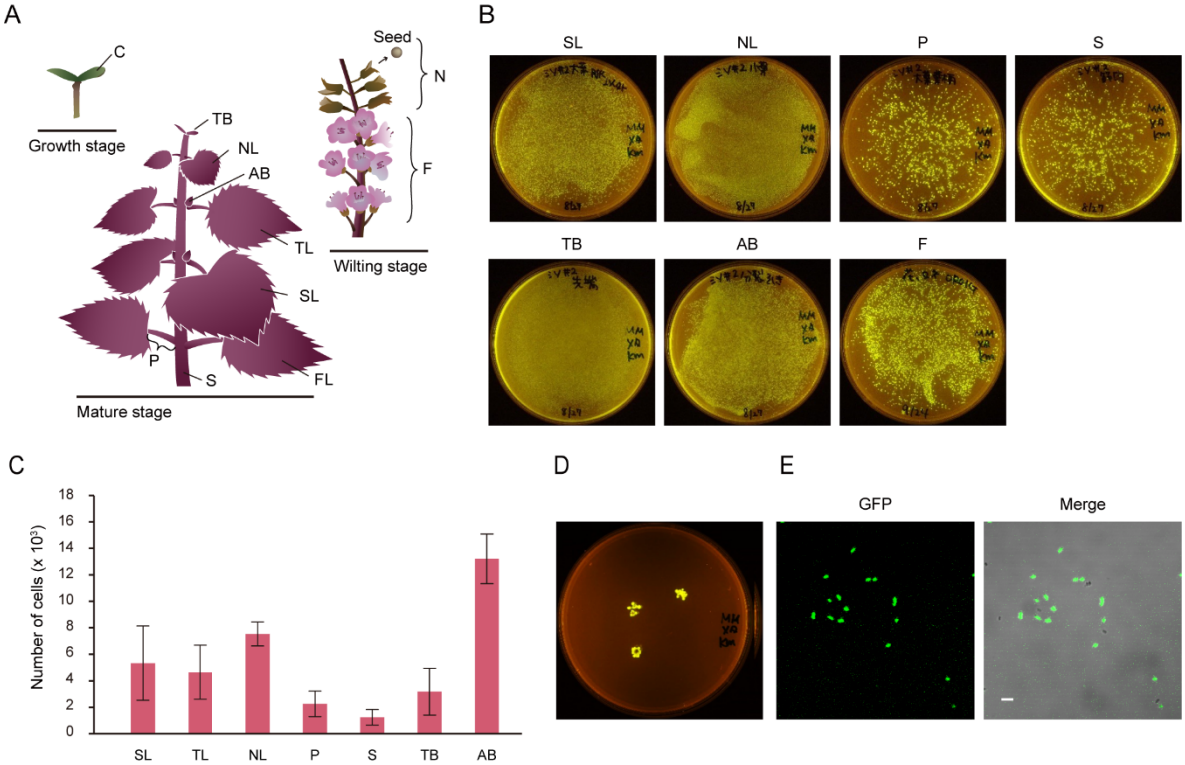

Fig. 1: Colonization of *Methylobacterium* sp. strain OR01 from seeds to whole plant of red perilla through plant surface.

A Schematic images of red perilla during plant development, i.e., growth, mature and wilting stages. C, cotyledon; TB, terminal bud; AB, axillary bud; P, petiole; S, stem; FL, first true leaf; SL, second true leaf; TL, third true leaf; NL, newest leaf; F, flower and N, next-generation seeds.

B Colony formation activity of the strain OR01-GFP collected from various parts of red perilla. Plant samples were harvested and suspended in sterile water. The bacterial cell suspension was spread onto hypho miminal agar plates supplemented with 0.5% methanol. Strain OR01-GFP was detected by FAS-Digi imaging system after 2–3 days.

C Quantitation of cell populations of strain OR01-mCherry on red perilla by FCM. Values are indicated as the number of cells per mg of plant sample and are shown as mean ± standard error of the mean (s.e.m.) of at least three independent measurements.

D The presence of strain OR01-GFP on next-generation seeds. Next-generation seeds were directly placed on hypho minimal agar plates and observed by FAS-Digi imaging system after 3 days.

E Microscopic images of the strain OR01-GFP collected from next-generation seeds. Cells of strain OR01-GFP were isolated from the seeds used in (**D**) and placed onto a slide glass for observation. GFP-fluorescence image (left) and differential interference contrast (DIC) image were merged (right). Bar, 5 µm.

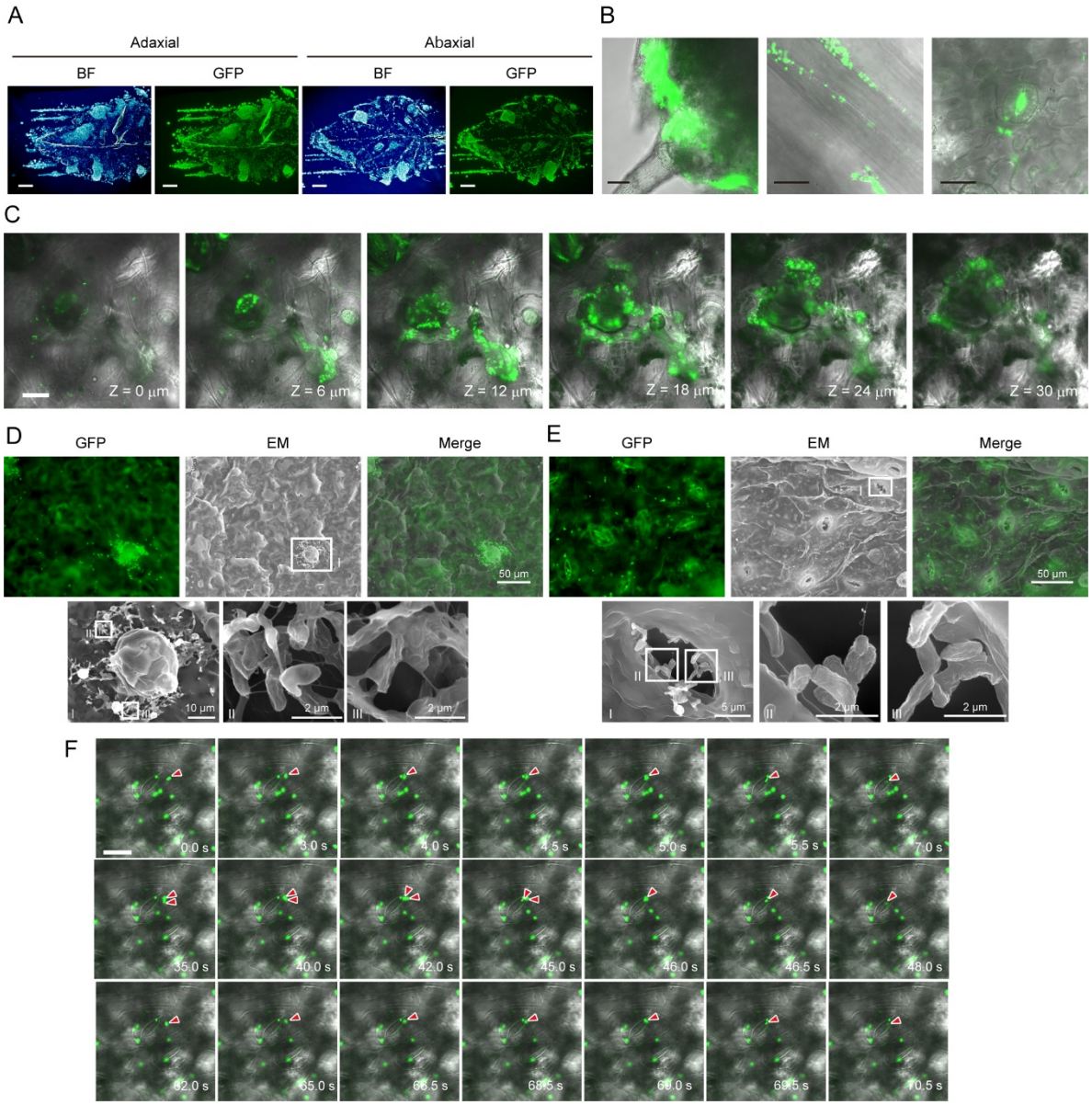

Fig. 2: Distribution of *Methylobacterium* sp. strain OR01 on red perilla leaves.

A Leaf-print assay of strain OR01-GFP on red perilla leaves at the adaxial side (left) and abaxial side (right). Bright-field (BF) image (left) and GFP-fluorescence image (right) are presented. Bar, 2 mm.

B Confocal fluorescence microscopic images showing strain OR01-GFP distributed at the base of the trichome (left), along the vein (central) and stomata (right). Bar, 20 µm.

C Z-stack images of stomata with strain OR01-GFP taken by a confocal fluorescence microscope (see also Supplementary Movie 1). Every next image from the left to the right was taken at 6 µm deeper location compared to the previous one. Bar, 20 µm.

D-E CLEM images of strain OR01-GFP around the trichome (**D**) and stomata (**E**). GFP fluorescence images (upper left) and EM images (upper central) were used for merged CLEM images (upper right). The EM images highlighted with a square (I) were magnified (lower left). The areas marked as square (II) and (III) were further magnified ((II): lower central and (III) lower right), respectively). Bars show the indicated lengths.

F Time-lapse images of strain OR01-GFP entering the stomatal cavity. The video was taken by a confocal microscope and recorded for 77 seconds. 21 images extracted at the indicated time points are shown (see also Supplementary Movie 2). Red arrows indicate cells entering into the stomatal cavity from the surface of the leaf. Bar, 20 μm.

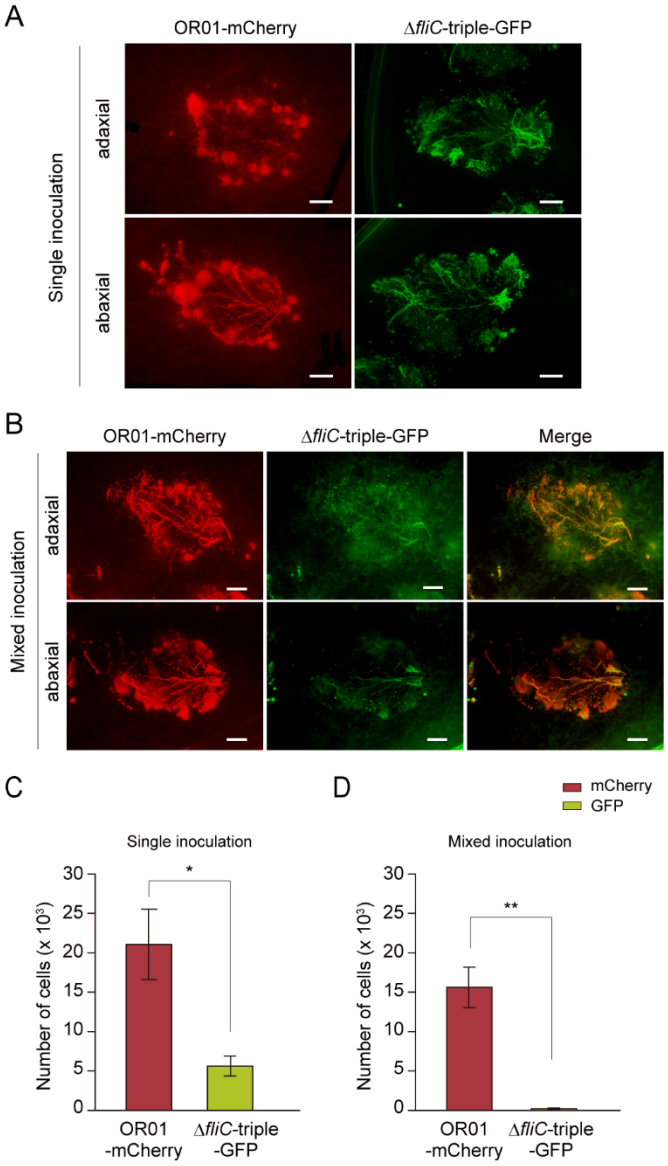

Fig 3: Colonization and distribution of FliC (flagellin)-deleted mutant of strain OR01 in the phyllosphere of red perilla.

A-B Visualization of colonization and distribution of strain OR01-mCherry and strain Δ*fliC*-triple-GFP on red perilla by leaf-print assay. Strain OR01-mCherry and strain Δ*fliC*-triple-GFP were inoculated in a single inoculum (**A**) or in a mixed inoculum (**B**). Bar, 2 mm.

C FCM-based quantification of cell populations of strain OR01-mCherry and strain Δ*fliC*-triple-GFP on red perilla. Values are indicated as the number of cells per mg of plant sample and are shown as mean ± s.e.m. of eight independent measurements. Asterisks indicate the level of statistical significance: ** $p < 0.01$, * $p < 0.05$.

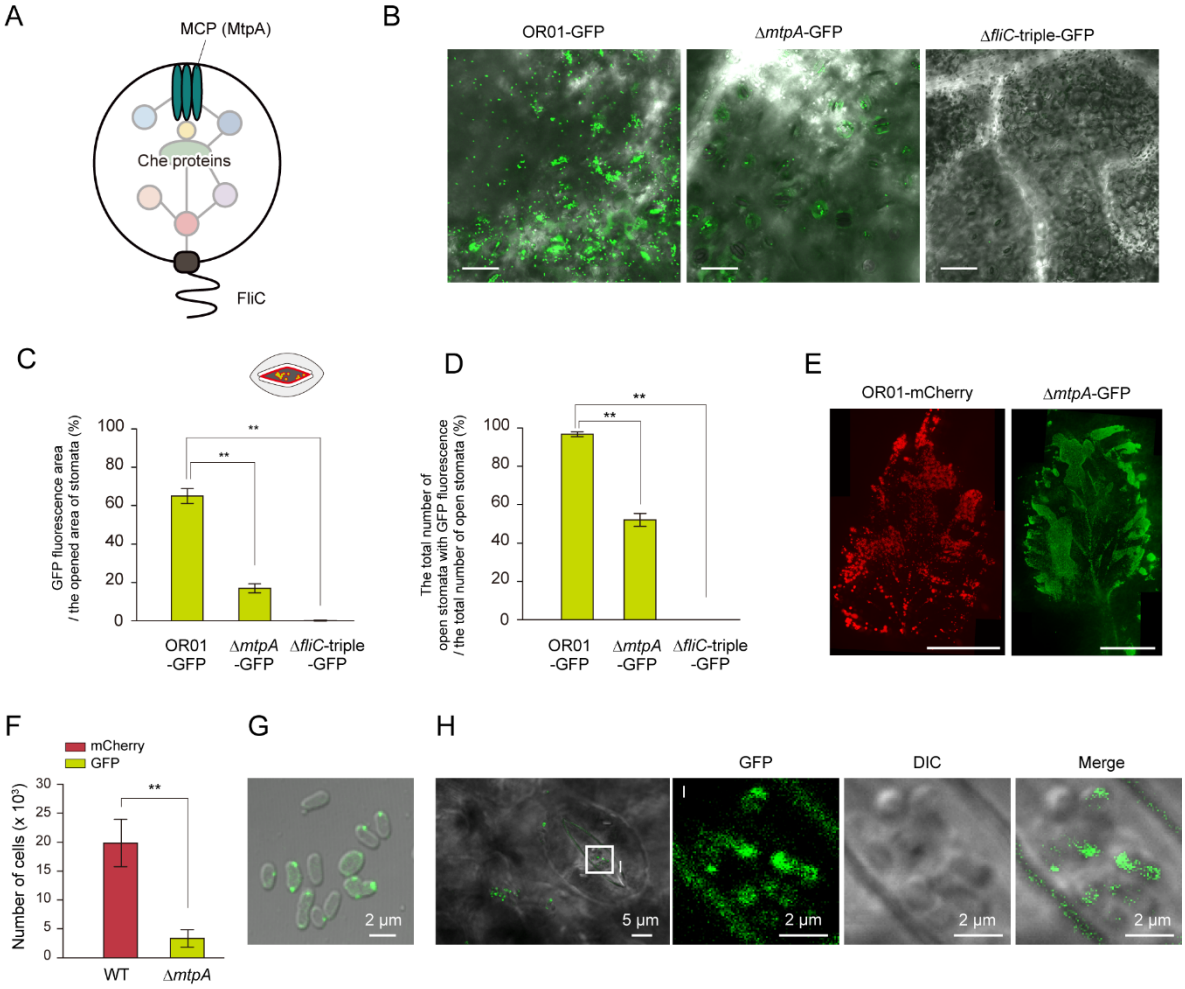

Fig 4: MtpA-dependent methylotaxis affected the distribution and colonization of strain OR01 in the phyllosphere of red perilla.

A Schematic diagram of the molecular mechanism of methylotaxis, consisting of methanol chemosensor MtpA, Che proteins and flagella (FliC).

B-D The strain OR01-GFP, strain Δ*mtpA*-GFP and strain Δ*fliC*-triple-GFP present in a single stoma. (**B**) Representative confocal microscopic images of strain OR01-GFP, strain Δ*mtpA*-GFP and strain Δ*fliC*-triple-GFP on red perilla leaves. Marged images of the DIC and GFP images are shown. Bar, 50 μm. (**C**) Quantification of the ratio of (area of the open stomata with GFP fluorescence) / (total area of open stomata) (%). Values are indicated as the number of cells per mg of plant sample and are shown as mean ± s.e.m. of the analysis of 18 stomata. Asterisks indicate the level of statistical significance between strain OR01-GFP and strain Δ*mtpA*-GFP, and strain OR01-mCherry and strain Δ*fliC*-triple-GFP: * $p < 0.05$, ** $p < 0.01$. (**D**) Quantification of the ratio of (number of open stomata with GFP fluorescence) / (number of all open stomata) (%). Values are indicated as the number of cells per mg of plant sample and are shown as the mean ± s.e.m. of the analysis of 60 stomata. Asterisks indicate the level

of statistical significance between strain OR01-GFP and strain Δ*mtpA*-GFP, and strain OR01-GFP and strain Δ*fliC*-triple-GFP: ** $p < 0.01$.

E Leaf-print assay of strain OR01-mCherry and strain Δ*mtpA*-GFP on the second true leaves of red perilla. Strain OR01-mCherry and strain Δ*mtpA*-GFP were inoculated in a single inoculum. Four to six images were combined by ImageJ plug-in MosaicJ for representative images. Bar, 1 cm.

F FCM-based quantification of cell populations of strain OR01-mCherry and strain Δ*mtpA*-GFP on red perilla. Values are indicated as the number of cells per mg of plant sample and are shown as mean ± s.e.m. of six independent measurements. Asterisks indicate the level of statistical significance between strain OR01-GFP and strain Δ*mtpA*-GFP: ** $p < 0.01$.

G Confocal microscopic images of strain Δ*mtpA*-GFP-MtpA. Cells were cultured on hypho minimal medium containing methanol as a carbon source. Marged image of the DIC and GFP images is shown. Bar, 2 μm.

H Confocal microscopic images of strain Δ*mtpA*-GFP-MtpA on the red perilla leaf surface. The original DIC- and GFP-merged image is shown (left). The highlighted square (I) is magnified, and shown with GFP, DIC, and merged images. Bars show the indicated lengths.

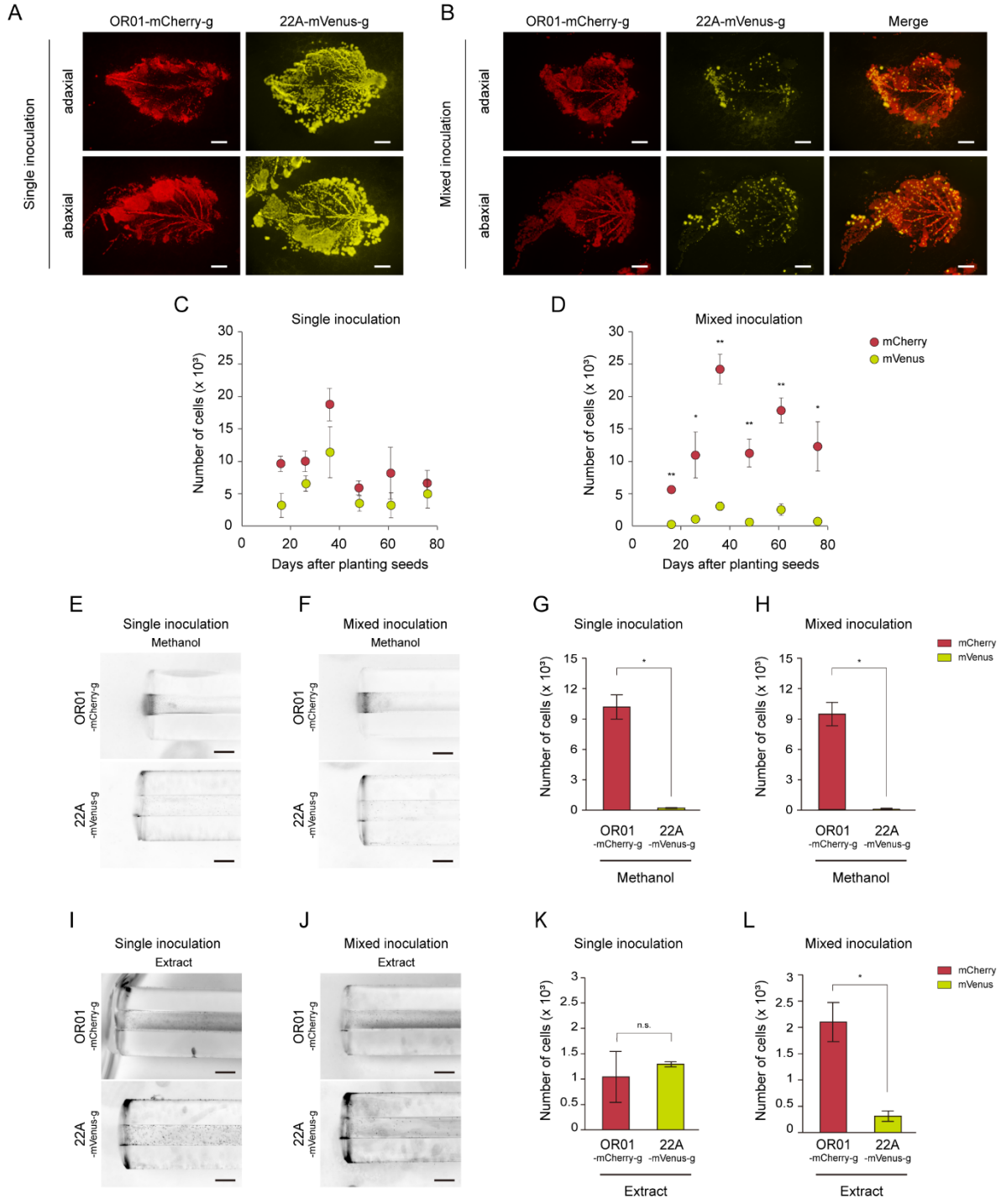

Fig 5: Competitive colonization analysis between strain OR01 and strain 22A on red perilla.

A-B Leaf-print assay of strain OR01-mCherry-g and strain 22A-mVenus-g on red perilla

leaves. These strains were inoculated in a single inoculum (**A**) or a mixed inoculum (**B**). Bar, 2 mm.

C-D FCM-based quantification of the cell populations of strain OR01-mCherry-g and strain 22A-mVenu-g on red perilla leaves. The first to third true leaves were harvested 16, 26, 36, 48, 61 and 78 days after seed planting with the inoculation of bacterial cells. Strain OR01-mCherry-g and strain 22A-mVenus-g were inoculated in a single inoculum (**C**) or in a mixed inoculum (**D**). Values are indicated as the number of cells per mg of plant sample and are shown as mean ± s.e.m. of at least three independent measurements. Asterisks indicate the level of statistical significance between strain OR01-mCherry-g and strain 22A-mVenu-g on each indicated date: ** $p < 0.01$, * $p < 0.05$.

E-H Capillary assay for methylotaxis of strain OR01-mCherry-g and strain 22A-mVenus-g. (**E-F**) The strains were placed close to the capillaries that contained a hypho minimal medium supplemented with 0.05 % methanol. The strains were inoculated in a single inoculum (**E**) or in a mixed inoculum (**F**). Images were taken by a stereo microscope. Bar, 200 µm. (**G-H**) FCM-based quantification of cell populations of strain OR01-mCherry-g and strain 22A-mVenus-g in capillaries. The strains were inoculated in a single inoculum (**G**) or in a mixed inoculum (**H**). Values are indicated as the number of cells per capillary and are shown as mean ± s.e.m. of three independent measurements. Asterisks indicate level of statistical significance between strain OR01-mCherry-g and strain 22A-mVenus-g: * $p < 0.05$.

I-L Capillary assay for chemotactic response of strain OR01-mCherry-g and strain 22A-mVenus-g to red perilla extract. (**I-J**) The strains were placed close to the capillaries that contain a hypho minimal medium supplemented with 0.4% red perilla extract. The strains were inoculated in a single inoculum (**I**) or in a mixed inoculum (**J**). Images were taken by a stereo microscope. Bar, 200 µm. (**K-L**) FCM-based quantification of cell populations of strain OR01-mCherry-g and strain 22A-mVenus-g in capillaries. The strains were inoculated in a single inoculum (**K**) or in a mixed inoculum (**L**). Values are indicated as the number of cells per capillary and are shown as the mean ± s.e.m. of three independent measurements. Asterisks indicate the level of statistical significance between strain OR01-mCherry-g and strain 22A-mVenus-g: * $p < 0.05$. Not significant: n.s.

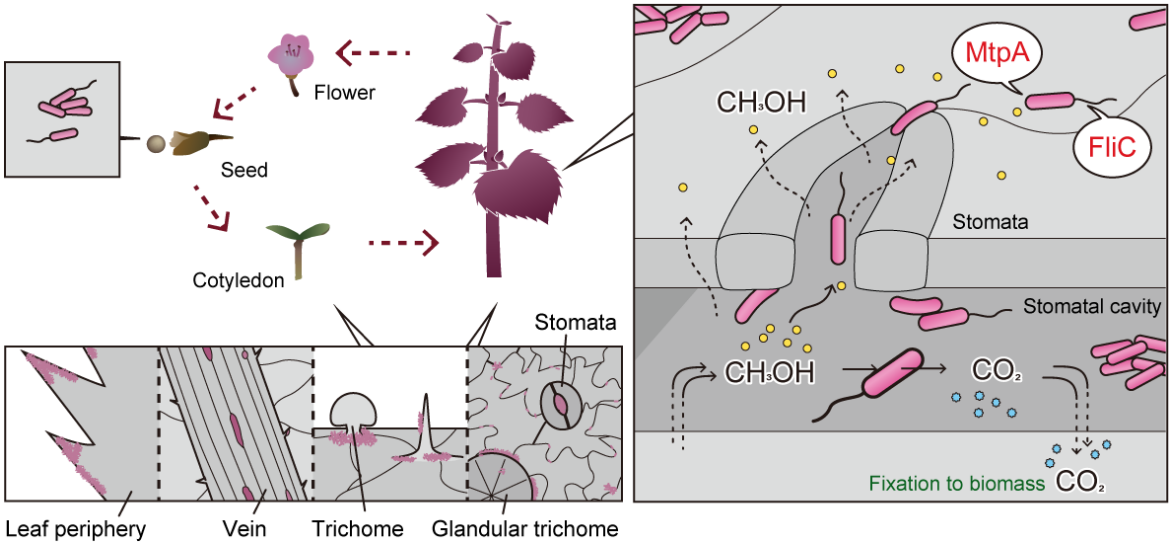

Fig 6: MtpA-dependent methylotaxis and FliC-driven motility enhance the colonization of *Methylobacterium* sp. strain OR-01 in the phyllosphere of red perilla. Strain OR01 travels throughout the plant surface in the phyllosphere and moves to seeds for the next generation concomitant with plant growth. Strain OR01 preferentially colonizes the leaf periphery, veins, trichomes and stomata. Methanol generated from pectin in the plant cell wall functions as a major volatile messenger to attract strain OR01 into the stomatal cavity aided by MtpA-driven methylotaxis and FliC-dependent motility. Within the stomatal cavity, strain OR01 oxidizes methanol to CO_2, resulting in an increase in CO_2 concentration used for photosynthesis by the host plant.